PCCP

Analysis of multipath transmission of spin–spin coupling constants in cyclic compounds with the help of partially spin-polarized orbital contributions

Anan Wu and Dieter Cremer*

Department of Theoretical Chemistry, Göteborg University, Reutersgatan 2, S-41320, Göteborg, Sweden

Received 27th March 2003, Accepted 30th July 2003
First published as an Advance Article on the web 12th September 2003

The multipath spin–spin coupling mechanism in cyclic compounds leads to NMR spin–spin coupling constants (SSCCs) strongly deviating from normal SSCCs. This is shown for ^{n}J(CC), ^{n}J(CH), and ^{n}J(HH) coupling constants of cyclic and bicyclic compounds using the recently developed decomposition of of J into orbital contributions using orbital currents and partial spin polarization (J-**OC**-PSP). A typical multipath SSCC depends on a through-space part, two or more through-bond parts, and the path-path interaction part where the latter results from steric exchange repulsion between the bond paths. The sign and magnitude of the through-space contribution as well as the through-bond contributions can be predicted by analysis of the Fermi contact spin density distribution calculated from the localized molecular orbitals involved in the coupling mechanism. In this way, unusual SSCCs of cyclopropane and bicyclo[1.1.1]pentane are explained for the first time. Also, measured and calculated ^{2}J(CC) coupling constants of cyclopentane and tetrahydrofuran are shown to be averages over the pseudorotational motion of these ring molecules where each individual SSCC of a conformation passed in the pseudorotation is the sum of different path contributions. The three-bond path contributions dominate the ^{2}J(CC) coupling constants of the pseudorotating molecules and introduce its dependence on the pseudorotational phase angle.

I. Introduction

NMR spin–spin coupling constants (SSCCs) provide important information about the electronic structure, the geometry, and the conformation of a molecule.[1–4] Many models and concepts have been developed to unravel the relationship between SSCCs and structural or electronic properties. One of these is the concept of multipath coupling, which explains the existence of unexpectedly large SSCCs found in ring compounds as a result of the existence of several paths, either through-bond (THB) or through-space (THS), by which spin polarization can be transmitted between two coupling nuclei.[4,5] A number of experimental and theoretical investigations has lent support to the concept of multipath coupling in cyclic and multicyclic compounds and, as such, it has gained general acceptance.[4–17] The question of the additivity of the individual components of the multipath mechanism, in order to obtain the total SSCC, is not a trivial one. Whereas early work assumed additivity to be fulfilled in most cases,[7–15] latter work showed that cases of both additivity and non-additivity can be found.[16] The multipath coupling mechanism includes a through-space component, which is difficult to predict on the basis of empirical estimates and therefore requires reliable quantum chemical calculations. The cases of nonadditivity are caused by exchange interactions between the various paths and again these interactions will be difficult to estimate if not quantum chemical methods are used that reliably reproduce the various path contributions.

The concept of multipath coupling heavily depends on the use of an accurate theory to calculate SSCCs. A second prerequisite is the existence of a method that decomposes the calculated SSCCs into path contributions. For a long time the first requirement was not fulfilled as semiempirical or non-empirical Hartree–Fock (HF) based methods used to calculate the SSCCs did not include a sufficient amount of electron correlation to obtain reliable SSCC values.[18,19] Multiconfigurational SCF (MCSCF) and coupled cluster (CC) methods for the calculation of SSCCs[20,21] are largely reliable, although they are too expensive to be routinely applied to larger rings systems with interesting multipath coupling. A solution to this methodological problem is offered by the coupled perturbed density functional theory (CP-DFT) approach,[22] which provides all terms of the indirect scalar SSCC according to the Ramsey theory[23] with sufficient accuracy when carried out with the hybrid functional B3LYP.[24] As the exchange functional used in B3LYP includes also nondynamic electron correlation,[25] CP-DFT performs almost as good as MCSCF or CCSD while having at the same time the advantage of being an economic method. As such, CP-DFT as developed by Cremer and co-workers[22] is the tool of choice for investigating multipath coupling in relatively large molecules.

The most advanced work on multipath coupling was performed by Contreras and co-workers,[5,13–16] who used the *inner projections of the polarization propagator* (*IPPP*)[18] approach for the analysis of transmission mechanisms. This was done initially in connection with the semiempirical intermediate neglect of differential overlap (INDO) approximation[13–15] and later IPPP was extended to an HF ground state wavefunction.[16] Despite the fact that none of the underlying methods could fulfill the requirements for calculating reliable SSCCs, the IPPP approach of Contreras and co-workers[18] provided for the first time reasonable explanations for multipath coupling, additivity and non-additivity, and the through-space component of multipath coupling.[13–16]

In this work, we investigate multipath coupling for the first time using CP-DFT to the extent that all Ramsey

contributions to the indirect isotropic SSCC (Fermi contact (FC), diamagnetic spin–orbit (DSO), paramagnetic spin–orbit (PSO), and spin–dipole (SD) terms[23]) are calculated,[22] which has not been done in previous work. As such, reliable total SSCCs and reliable path contributions can be expected for all the molecules considered in this work. Furthermore, we apply the recently developed decomposition of of J into orbital contributions using orbital currents and partial spin polarization (J-OC-OC-PSP = J-**OC**-PSP)[26] to analyze the multipath SSCCs. The basic idea of J-**OC**-PSP is to calculate the SSCC by imposing restrictions on the spin polarization within a set of localized molecular orbitals (LMOs), which correspond to a given molecular fragment. In this way, all other contributions to the SSCC in question are discarded and only those contributions to the SSCC associated with the molecular fragment of interest are considered. Each LMO contribution to the SSCC (or to FC, PSO, DSO, and SD term) represents either repolarization or delocalization of the spin density transmitting the coupling mechanism. Steric exchange interactions between the LMOs lead to further contributions to the SSCC. Each of these LMO contributions and the corresponding spin polarization can be related to typical features of the electronic structure as we have demonstrated in two recent publications.[26,27]

We will show that J-**OC**-PSP in connection with CP-DFT provides a clear picture of multipath coupling and answers the additivity/non-additivity question in an unique way. Sign and magnitude of the multipath SSCCs can be rationalized using the spin density distribution calculated with the associated LMOs. Consequently, the importance of through-space paths and path interactions can be described in detail. We make an additional step by demonstrating the role of multipath coupling for conformationally highly flexible molecules such as pseudorotating five-membered rings. In such cases one can obtain experimentally only one SSCC value, which is the weighted average over all individual SSCCs J associated with a given conformation of the ring populated during ring pseudorotation. Each of the individual J values contributing to the measured average value $\langle J\rangle$ comprises the sum of various path contributions, so that the rationalization of sign and magnitude of the measured SSCC becomes extremely difficult. We will show in this work that theory provides the tools to unravel the various relationships.

II. Theory of the J-OC-PSP method

According to the theory of magnetic indirect spin–spin coupling as formulated by Ramsey,[23] the coupling interaction can be expressed in terms of Hamiltonian (1):

$$\hat{H} = \hat{H}_{1a} + \hat{H}_{1b} + \hat{H}_2 + \hat{H}_3 \tag{1}$$

where $\hat{H}_{1a}$ and $\hat{H}_{1b}$ describe the DSO and PSO interactions, $\hat{H}_2$ the SD and $\hat{H}_3$ the FC interactions between the coupling nuclei. Applying the Hamiltonian in eqn. (1) and utilizing Kohn–Sham DFT,[28] the four contributions to the indirect scalar SSCC can be given by eqns. (2a)–(2d):[22]

$$K_{AB}^{DSO} = \frac{2}{3}\sum_{k}^{occ}\left\langle \phi_k^{(0)}\middle|\,\mathrm{Tr}\,\boldsymbol{h}_{AB}^{DSO}\middle|\phi_k^{(0)}\right\rangle \tag{2a}$$

$$K_{AB}^{PSO} = -\frac{4}{3}\sum_{k}^{occ}\left\langle \phi_k^{(0)}\middle|\boldsymbol{h}_{A}^{PSO}\middle|\phi_k^{(B),PSO}\right\rangle \tag{2b}$$

$$K_{AB}^{FC} = \frac{2}{3}\sum_{k\sigma}^{occ}\left\langle \psi_{k\sigma}^{(0)}\middle|\boldsymbol{h}_{A}^{FC}\middle|\psi_{k\sigma}^{(B),FC}\right\rangle \tag{2c}$$

$$K_{AB}^{SD} = \frac{2}{3}\sum_{k\sigma}^{occ}\left\langle \psi_{k\sigma}^{(0)}\middle|\boldsymbol{h}_{A}^{SD}\middle|\psi_{k\sigma}^{(B),SD}\right\rangle \tag{2d}$$

where $\phi_k^{(B),X}$ and $\psi_{k\sigma}^{(B),X}$ correspond to the first order space and spin orbitals, respectively. In the following derivation we consider just the spin orbitals needed for the FC and SD terms. Similar formulas apply to the PSO term expressed in space orbitals. Discussion of the DSO term (also expressed in space orbitals) is not necessary because its decomposition into orbital contributions is straightforward as reflected by eqn. (2a). The first-order spin orbitals $\psi_{k\sigma}^{(B),X}$ are given by

$$\left|\psi_{k\sigma}^{(B),X}\right\rangle = \sum_{a\sigma'}^{virt}\frac{\left\langle \psi_{a\sigma'}^{(0)}\middle|\boldsymbol{F}_B^X\middle|\psi_{k\sigma}^{(0)}\right\rangle}{\varepsilon_k - \varepsilon_a}\left|\psi_{a\sigma'}^{(0)}\right\rangle \tag{3}$$

The symbol X stands for PSO, FC or SD, indices k and a denote occupied and virtual orbitals, respectively while σ and σ' are spin variables. Operator $\boldsymbol{F}_B^X$ depends on the first-order spin orbital $\psi_{k\sigma}^{(B),X}$ (first order space orbitals $\phi_k^{(B),X}$) in a similar way as the KS operator $\boldsymbol{F}$ depends on the KS orbitals.

$$\boldsymbol{F}_B^X = \boldsymbol{h}_B^X + \tilde{\boldsymbol{F}}_B^X \tag{4a}$$

$$\tilde{\boldsymbol{F}}_B^X = \sum_{k\sigma}^{occ}\int \mathrm{d}^3 r\frac{\delta \boldsymbol{F}_B^X}{\delta\psi_{k\sigma}(\boldsymbol{r})}\psi_{k\sigma}^{(B),X} = \sum_{k}^{occ}\tilde{\boldsymbol{F}}_B^{k,X} \tag{4b}$$

For the PSO, FC, and SD terms, eqns. (2a)–(2d) can be rewritten according to eqn. (5):

$$K_{AB}^X = C\sum_{k\sigma}^{occ}\sum_{a\sigma'}^{virt}\left\langle \psi_{k\sigma}^{(0)}\middle|\hat{\boldsymbol{h}}_A^X\middle|\psi_{a\sigma'}^{(0)}\right\rangle\frac{\left\langle \psi_{a\sigma'}^{(0)}\middle|\tilde{\boldsymbol{F}}_B^X\middle|\psi_{k\sigma}^{(0)}\right\rangle}{\varepsilon_a - \varepsilon_k} \tag{5}$$

where the pre-factor C is $-4/3$ for the PSO, $2/3$ for the FC and SD terms; ε_k and ε_a are the orbital energies of occupied and virtual orbitals, respectively. For the analysis of K in terms of orbital contributions, it is useful to use localized molecular orbitals (LMOs) η_i (although this analysis can be carried out with any type of orbital). Canonical orbitals and LMOs are connected by an unitary transformation according to eqn. (6).

$$\psi_{ma} = \sum_{i}^{occ} c_{mi}^{\sigma}\eta_{i\sigma} \tag{6}$$

By substituting eqn. (6) into eqn. (5) one obtains eqn. (7).

$$K_{AB}^X = C\sum_{i\sigma}^{occ}\sum_{a\sigma'}^{virt}\left\langle \eta_{i\sigma}^{(0)}\middle|\hat{\boldsymbol{h}}_A^X\middle|\psi_{a\sigma'}^{(0)}\right\rangle\sum_{j\sigma}^{occ}\sum_{k\sigma}^{occ}c_{ki}^{\sigma}c_{kj}^{\sigma} \times\frac{<\psi_{a\sigma'}^{(0)}\middle|\tilde{\boldsymbol{F}}_B^X\middle|\eta_{j\sigma}^{(0)}>}{\varepsilon_a - \varepsilon_k} \tag{7}$$

In eqn. (7) it is considered that the use of localized orbitals in the virtual space is unnecessary because the sum over all virtual orbitals rather than any individual virtual orbital is required. The first order LMO $\eta_i^{(1)}$ is given by eqn. (8):

$$\eta_{i\sigma}^{(1)} = \sum_{a\sigma'}^{virt}\sum_{j\sigma}^{occ}\sum_{k\sigma}^{occ}c_{ki}^{\sigma}c_{kj}^{\sigma}\frac{\left\langle \psi_{a\sigma'}^{(0)}\middle|\tilde{\boldsymbol{F}}_B^X\middle|\eta_{j\sigma}^{(0)}\right\rangle}{\varepsilon_a - \varepsilon_k}\left|\psi_{a\sigma'}^{(0)}\right\rangle \tag{8}$$

In eqn. (4b) it is indicated that the first order perturbation operator can be decomposed into orbital contributions, which does not change when LMOs are used:

$$\tilde{\boldsymbol{F}}_B^X = \sum_{i}^{occ}\tilde{\boldsymbol{F}}_B^{i,X} \tag{9}$$

Accordingly, the PSO, FC, and SD terms K_{AB}^X can be split up into one- and two orbital terms.[26,27]

$$K_{AB}^{i,X} = \langle\eta_i|\hat{\boldsymbol{h}}_A^X|\eta_i^{(1)}(F_i)\rangle \tag{10a}$$

$$K_{AB}^{ij,X} = \langle\eta_j|\hat{\boldsymbol{h}}_A^X|\eta_j^{(1)}(F_i)\rangle \tag{10b}$$

Eqn. (10a) describes the relaxation of an orbital under the impact of a magnetic perturbation at nucleus B. This

relaxation can be connected with a repolarization of charge in orbital η_i(excitation $\eta_i \rightarrow \eta_i^*$ where η_i^* is the to η_i associated antibonding LMO) or delocalization of charge into another orbital described by the excitation $\eta_i \rightarrow \eta_j^*$. Eqn. (10b) corresponds to a steric exchange interaction between occupied LMOs η_i and $\eta_j^{(1)}$. The notations $\eta_i^{(1)}(F_i)$ and $\eta_j^{(1)}(F_i)$ indicate that the spin–spin transmission mechanism is initialized by polarizing (perturbed) LMO η_i alone (the polarization of all other orbitals is set to zero). In this way, the different effects of the LMOs on the spin–spin coupling mechanism are separated.

By using LMOs, the set of orbitals can be partitioned into subspaces containing all bond (bd) LMOs, which directly connect the coupling nuclei, all lone pair (lp) LMOs associated with the coupling nuclei, and all core (c) LMOs of the coupling nuclei. Bond orbitals not included in the direct bond path between the coupling nuclei (*e.g.* C–H bond orbitals for a CC coupling path) are collected in the set of *other bond* (ob) LMOs. In this way, different transmission mechanisms associated with different coupling paths each given by a specific set of LMOs can be identified. In this work, we will apply the ***J*-OC-PSP** approach for the analysis of multipath spin–spin coupling mechanisms.

III. Computational methods

In this work, the molecules shown in Scheme 1 were investigated. Their geometries were optimized with DFT/B3LYP[24] using Pople's 6-31G(d,p) basis set[29] and, in the case of cyclopentane and tetrahydrofuran (THF), in addition with second-order many-body perturbation theory (MBPT2) using the Møller–Plesset (MP) perturbation operator[30] and Dunning's cc-pVTZ basis set.[31] The conformational energy surfaces (CES) of cyclopentane and THF were calculated by using the puckering coordinates developed by Cremer and Pople.[32–34]

The SSCCs were determined using CP-DFT as recently described by Cremer and co-workers.[22] It has been shown that reliable SSCC values are obtained with the B3LYP functional.[24,35,36] In this work, the B3LYP functional was employed in connection with the (9s,5p,1d/5s,1p)[6s,4p,1d/3s,1p] basis set designed for the calculation of magnetic properties.[37] All SSCC calculations were carried out with the *ab initio* program package COLOGNE 2003[38] while the geometry optimizations were done with Gaussian 98.[39].

The multipath contributions were calculated within the ***J*-OC-PSP** approach[26] also programmed for COLOGNE 2003. For the cyclic compounds, different coupling paths are defined as illustrated in Fig. 1:

(a) Through-bond paths (THB paths): They are formed by the ring bonds and other bonds along the corresponding path. For the geminal SSCC ^2J(C1C3) in cyclopentane, there is a two-bond path (clockwise around the ring perimeter, Fig. 1a) and a three-bond path (counterclockwise around the ring perimeter, Fig. 1b). They are described by the corresponding CC bond LMOs. However, for the spin–spin coupling mechanism, one has to consider beside the corresponding σ(CC) LMOs also the σ(CH) LMOs in each path because spin polarization can be transferred not only *via* the σ(C1C2) - σ(C2C3) two-bond path but also *via* the σ(C1H6) - σ(C1C2), σ(C1H6) - σ(C2C3) subpaths and all possible similar subpaths. Inclusion of the σ(CH) LMOs (or lp(O) LMOs in the case of THF) leads also to through-space contributions, which have to be calculated separately (see b) and deducted from the calculated THB contributions to obtain the THS-free path contributions.

b) Through-space paths (THS paths): This path includes all through-space subpaths between the LMOs of the coupling nuclei (*e.g.* C1 and C3 in Fig. 1c) with the exception of the ring bond LMOs, but including the core orbitals of the coupling nuclei. For example, one important contribution to the THS path results from the steric exchange interaction of the CH LMOs (or a lp(O) LMO and a CH bond LMO in the case of THF).

c) Path interactions (PI): Steric exchange interactions between the ring bond LMOs are not covered in b), but they can lead to substantial contributions to the coupling mechanism thus destroying the additivity of path increments. Therefore they are summarized in the PI contribution, which is obtained as a difference between the total SSCC and the sum of THS + THB contributions.

All SSCCs investigated in this work for the molecules shown in Scheme 1 were partitioned according to a), b), and c) and will be discussed in the next chapter.

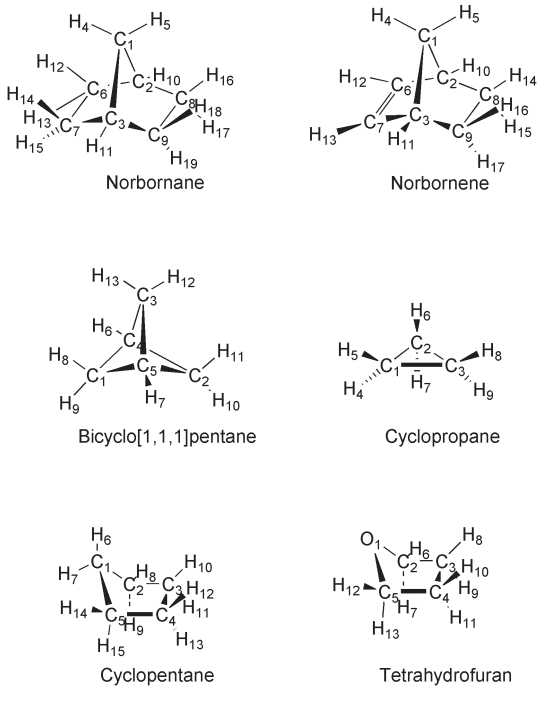

Scheme 1

IV. The mechanism of spin–spin multipath coupling

In Table 1, some typical multipath SSCCs are listed for bicyclic compounds such as bicyclo[1.1.1]pentane, norbornane or norbornene. Calculated SSCCs agree with the few experimental data available (given in Table 1 in parentheses), which are due to substituted systems. The SSCC J(C2C3) of norbornane with CO_2H at the bridgeatom was measured to be 7.38 Hz[4] in good agreement with the value obtained in this work (7.60 Hz, Table 1). In norbornane itself, J(C2H11) was found to be 8.7 Hz[41] in perfect agreement with the calculated value (8.68 Hz, Table 1). Similarly, the measured SSCC J(C4C5) of bicyclo[1.1.1]pentane (±25.16 Hz[4]) is close to the calculated value of −26.11 Hz (Table 1). For cyclopropane, the J(CC) value of 12.4 Hz[40] is well reproduced by theory (12.9 Hz, Table 1). We note that different SSCC values will be obtained if one of the coupling paths carries additional substituents because these bonds participate in the coupling mechanism and, accordingly, change multipath spin–spin coupling. Examples can be found in the compilations of Marshall,[42] Marchand,[43] and Krivdin and Della.[4]

Apart for the ^1J(CC) constant in bicyclo[1.1.1]pentane and in cyclopropane (case B in Table 1), which was included for reasons discussed later, all multipath SSCCs investigated fulfil the additivity rule within ±0.5 Hz. There are some PI contributions for the SSCCs J(CC) (0.55 Hz) and J(CH) (−0.36 Hz, Table 1) of norbornene, however these contributions are still

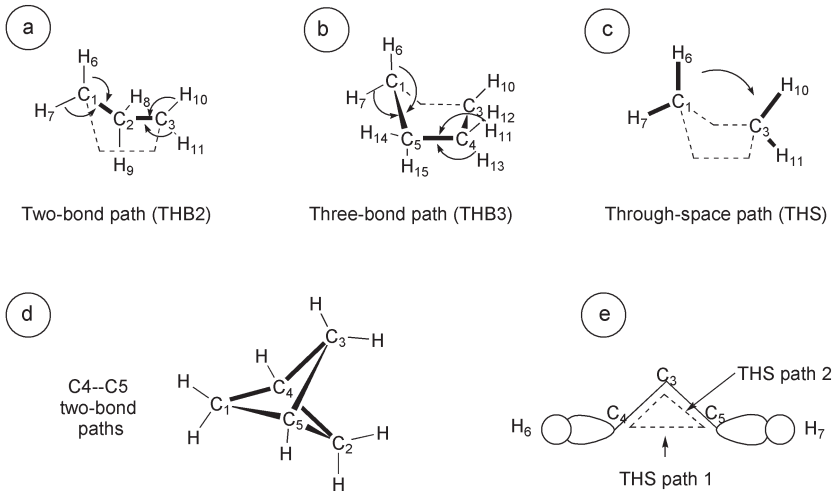

Fig. 1 Explanation of different path contributions in cyclopentane and bicyclo [1.1.1]pentane. (a) Two-bond path, (b) three-bond path, and (c) through-space path for $J(C1C3)$ in cyclopentane. The thick solid lines indicate the CC THB-paths. Arrows indicate that contributions from the CH bonds have to be considered. (d) The three two-bond paths for $J(C4C5)$ in bicyclo [1.1.1]pentane. (d) The through-space (THS) interaction between C4 and C5 in bicyclo [1.1.1]pentane splits up into THS path 1 and THS path 2 (compare with Fig. 2a).

small compared to the other contributions so that it is justified to speak of path additivity. This result is in line with semiempirical and HF work carried out by Contreras and co-workers.[13–16]

Results for the bicyclic compounds show that it should be possible to define increments for the various path contributions only if the molecules under consideration possess closely related structures so that the THS contributions do not change significantly (compare norbornane and norbornene in Table 1). If this is not the case, the strong variation in the THS contributions makes it difficult, if not impossible, to cover THS effects by defining suitable increments on the basis of empirical rules and measured SSCCs. Theory shows that the THS increments can have both negative and positive sign and that their magnitude may be as large as 11 Hz (bicyclo[1.1.1]pentane, Table 1). ***J*-OC-PSP** makes it possible to analyze the trends in THB and THS contributions, which are dominated by the FC term of the SSCC. Fig. 2a shows a contour line plot of the zeroth order LMOs $\sigma(C4H6)+\sigma(C5H7)$ of bicyclo[1.1.1]pentane and Fig. 2b the corresponding Fermi contact spin density distribution,[26] which results from the combination of the products of the zeroth order LMOs and the corresponding first order orbitals with a perturbation at H6 (Fig. 2b: lower H nucleus). Solid contour lines are in regions of a dominance of α-spin density, dashed contour lines in a region of a dominance of β-spin density.

Table 1 Decomposition of NMR spin–spin coupling constants ^nJ(CC) and ^nJ(HH) resulting from a multipath mechanism into different path contributions[a]

Molecule	Type	J(THS)	^nJ(Path 1)	^nJ(Path 2)	^nJ(Path 3)	$\sum$	PI	Total
Class A								
Bicyclo[1.1.1]pentane		THS	^3J	^3J	^3J			
	C4H7	−3.06	5.59	5.59	5.59	13.71	−0.18	13.53
		THS	^4J	^4J	^4J			
	H6H7	10.71	1.15	1.15	1.15	14.15	0.04	14.19
Norbornane		THS	^2J	^3J	^3J			
	C2C3	−4.94	−2.46	7.52	7.52	7.64	−0.04	7.60 (7.38[d])
		THS	^3J	^4J	^4J			
	C2H11	1.50	5.91	0.84	0.84	9.08	−0.40	8.68 (8.7[d])
		THS	^4J	^5J	^5J			
	H10H11	0.20	0.03	−0.08	−0.08	0.08	0.06	0.14
Norbornene		THS	^2J	$^3J^b$	$^3J^c$			
	C2C3	−4.88	−3.04	7.62	6.94	6.65	0.55	7.20
		THS	^3J	$^4J^b$	$^4J^c$			
	C2H11	1.29	6.23	0.98	0.52	9.02	−0.36	8.66
		THS	^4J	$^5J^b$	$^5J^c$			
	H10H11	0.55	0.10	−0.11	−0.11	0.43	0.06	0.49
Class B								
Bicyclo[1,1,1]pentane		THS	^2J	^2J	^2J			
	C4C5	−2.58	−4.44	−4.44	−4.44	−15.90	−10.21	−26.11 (±25.16[d])
Cyclopropane		THS	^{1}J	^2J				
	C1C2	−27.08	54.39	10.08		37.39	−24.48	12.91 (12.4[d])

[a] All values in Hz. For a numbering of atoms, compare with Scheme 1. THS gives the through-space contribution, path n the through-bond contribution n while $\sum$ stands for the sum of THS and THB contributions. PI gives the contribution resulting from the interactions between different paths. [b] The ^3J path *via* the CC single bond. [c] The ^3J path *via* the CC double bond. [d] Experimental values from ref. 4(norbornane, bicyclo[1.1.1]-pentane), 40 (cyclopropane), 41 (norbornane).

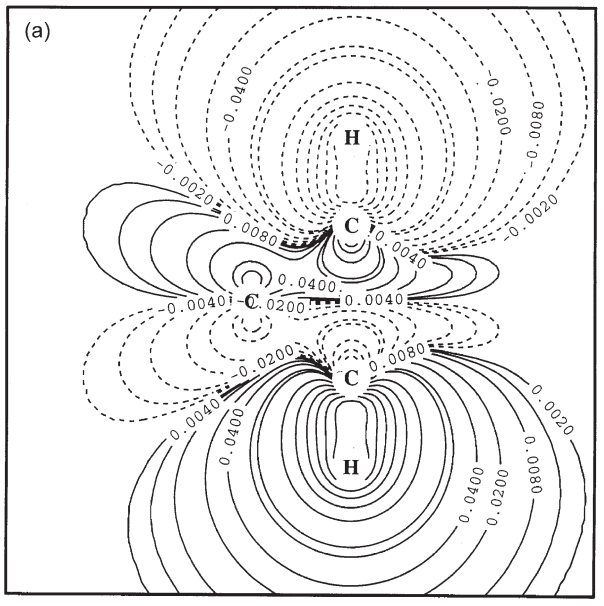

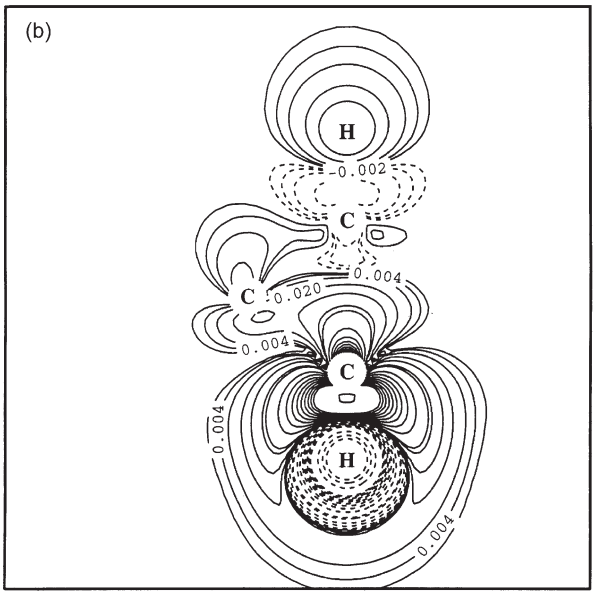

Fig. 2 (a) Contour line diagram of the zeroth order LMOs $\sigma(C4H6)+\sigma(C5H7)$ (C4H6 is the lower, C5H7 is the upper bond, bridge atom C3 is at the left; compare with Fig. 1e). (b) Contour line diagram of the Fermi contact spin density distribution resulting from the zeroth- and first-order σ(CH) bond orbitals involving C4H6 and C5H7. The perturbation is at the lower H atom, which corresponds to H6.

The back lobes of the $\sigma(CH)$ bond orbitals lead to a direct interaction through-space (indicated in Fig. 1e as THS path 1) and an indirect interaction in the region of the bridge C atom (indicated in Fig. 1e as THS path 2). The sign of the FC term as transmitted by the THS spin-polarization is determined by the sign of the FC spin density distribution at the coupling nuclei.[26] If the proton H6 (lower proton in Fig. 2) adopts α-spin, then the spin density is negative at this proton, positive at the bonded bridgehead C, positive at the bridge carbon, negative at the other bridgehead C, and positive on proton H7 (upper proton in Fig. 2). Due to Fermi coupling between nuclear spin and electron spin, this leads to a negative sign for ^2J(THS,C4H7) = ^2J(THS,C5H6)(−3.1 Hz) and a positive sign for ^3J(THS,H6H7)(10.7 Hz) whereas the through-space interaction can be formally counted as a one-bond interaction because of the relative large density between the bridgehead C atoms in bicyclo[1.1.1]pentane.

In a similar way one can show that the spin-density leads to a negative ^1J(THS,C4C5) value for bicyclo[1.1.1]pentane (−2.6 Hz, Table 1) when one of the bridgehead nuclei is perturbed. There seems to be a positive and a negative contribution to the THS part involving the bridgehead C atoms, namely the direct interaction between the back lobes of the σ(CH) bonding LMOs yielding a positive contribution (Fig. 1e, THS path 1; also Fig. 2a) and a second interaction including also the back lobes of the CH bond orbitals in the bridge, which leads to a negative contribution (Fig. 1e, right side, THS path 2; also Fig. 2a). The two contributions cancel each other partially so that a smaller negative value (−2.6 Hz) than in he cases of norbornane (−4.9 Hz) or norbornene (−4.9 Hz, Table 1) results for which the negative contribution should clearly dominate (because of the large bridgehead distance C···C decreasing the positive contribution from THS path 1).

The signs of the FC spin density distribution at the coupling nuclei can be predicted by inspection of the nodal behavior of zeroth and first order orbital, which determines the the relative signs of these orbitals at the nuclei (for a detailed discussion see refs. 26 and 27). Although the form of the first order orbitals depends on the nucleus perturbed, the product of the FC spin densities at the nuclei will have the same sign. The two-bond and three-bond path contributions have signs as one should expect for normal SSCCs. The three-bond path normally leads to the largest contribution since the topology of the bicyclic molecule forces the corresponding bonds into a *cis*-arrangement. Sizable contributions result also from the two-bond paths but these are, as normal geminal SSCCs ^2J(CC), all negative.[40] Contributions from the four- and five-bond paths are rather small (exception: bicyclo[1.1.1]pentane) and can have both signs (Table 1). In view of these partially opposing trends, it will be difficult to define suitable increments without appropriate calculations. Hence, the analysis of measured multipath SSCCs requires the application of theoretical methods such as the one used in this work.

Nonadditivity is found for the ^1J(CC) of bicyclo[1.1.1]pentane, which has a PI part of −10.2 Hz. This is a result of the structure of the molecule leading to a relatively strong interaction between the three bridges (Fig.1d). Obviously, the analysis of the multipath SSCC can reveal these interactions and therefore can be considered as a valuable tool for through-space and through-bond interactions.

Cyclopropane, although not a bicyclic molecule, is the simplest organic compound with a dual-pathway for $^{13}C,^{13}C$ coupling. Stöcker[17] suggested to take the ^1J(CC) value of ethane (34.6 Hz[40]) and to add an assumed ^2J(CC) value of −20 Hz so that a value close to the experimental cyclopropane SSCC ^1J(CC) of 12.4 Hz[17] is found. This approach however has to be criticized because it does not consider the difference in CC bonding between ethane and cyclopropane,[44] it does not include a THS contribution, which certainly exists (see Scheme 2), and it ignores the strong PI between the one-bond and the two-bond path.

The *J*-**OC**-PSP calculations reveal that the one-bond path contributes 54.4 Hz (Table 1), which is between ^1J(CC) of ethane (34.6 Hz) and ^1J(CC) of ethene (67.6 Hz[40]) in line with the known π-bond character of the CC bonds in cyclopropane. The two-bond path adds another 10.1 Hz (Table 1) typical of a geminal CC coupling in strained rings,[4,40] but with opposite sign. Actually, the two-bond path has to be seen together with the THS part of the SSCC (see Scheme 2), which is −27.1 Hz (Table 1) indicating that the interactions between the back-lobes of the CH hybrid orbitals through-space play an important role. The sum of these contributions (10.1 − 27.1 = −17 Hz) leads to a strongly negative contribution as one should expect for a ring with high strain. Finally, the interaction between one-bond and two-bond path adds another −24.5

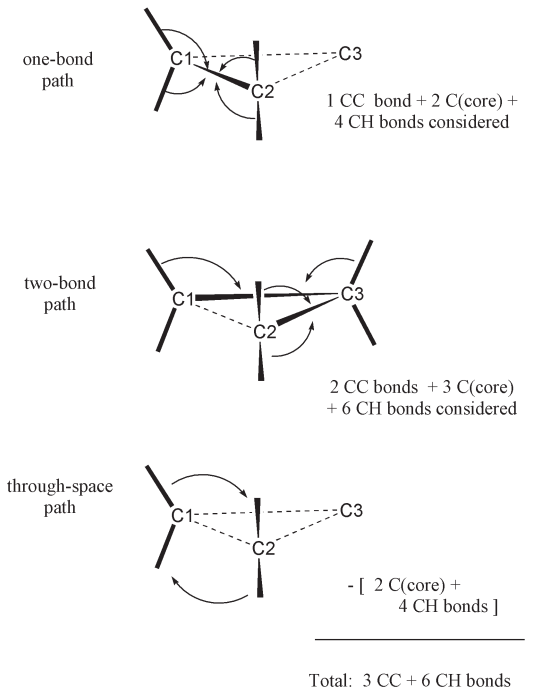

Scheme 2

Hz (Table 1) thus reducing the large one-bond path contribution to the relatively small total SSCC of 12.9 Hz (measured 12.4 Hz[40]). We conclude that electronic features of CC bonding in cyclopropane can only be assessed from the measured ^1J(CC) value if it is decomposed in a multipath analysis. The approach by Stöcker[17] was in this respect highly misleading.

An alternative decomposition of ^1J(CC) with the help of the canonical orbitals of cyclopropane is also interesting in this connection. The canonical orbitals exclude a multipath analysis because each orbital includes THB and THS parts. However, one can single out from the nine occupied valence orbitals just two orbitals ($2a'_1$ and one of the $2e'$) because for the other orbitals the C atoms are positioned in nodal planes and therefore a contribution to the FC term is not possible. The $2a'_1$ orbital is a CCC bonding orbital and it leads to a large positive contribution of 77.2 Hz to ^1J(CC). The $2e'$ orbital contributes −66.0 Hz thus reducing the contribution to 11.2 Hz already close to the actual value of 12.9 Hz (resulting from additional core contributions). By localization of the orbitals these two large contributions are split up into smaller contributions, which can be associated with certain coupling paths.

V. Multipath coupling in pseudorotating molecules

Puckered five-membered rings can undergo pseudorotation, which is best described using the Cremer–Pople puckering coordinates.[32–34] For a five-membered ring, these comprise the pseudorotational phase angle ϕ describing the mode of ring puckering and the puckering amplitude q describing the degree of ring puckering. An infinite number of ring conformations is located along the pseudorotational path, of which in the case of cyclopentane or THF a subset of 20 forms is easy to recognize because it comprises the ten envelope (E) forms ($\phi = (0+360k)/10$ for $k = 0,1,2,\ldots,9$) and the ten twist (T) forms ($\phi = (18+360k)/10$ for $k = 0,1,2,\ldots,9$) of a five-membered ring (see Fig. 3). The CES must comply with the

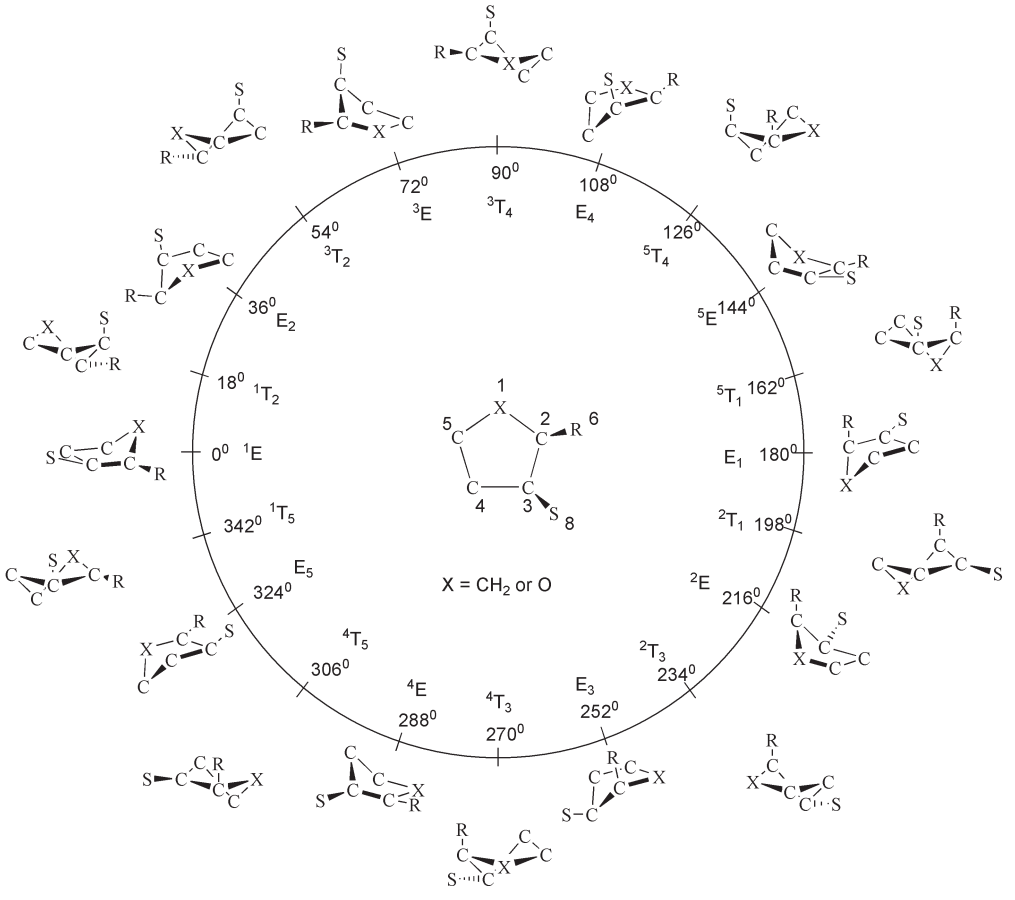

Fig. 3 Pseudorotation itinerary ($\phi = 0 \rightarrow 360°$) of cyclopentane (X = CH_2) and tetrahydrofuran (THF: X = O) as indicated by the 10 envelope (E) and ten twist (T) forms at $\phi = (0+360k)/10$ and $\phi = (18+360k)/10$ ($k = 0,1,2,\ldots,9$). At the center ($q = 0$), the planar ring is located. To distinguish different positions in the ring, symbols R, S are used for substituents.

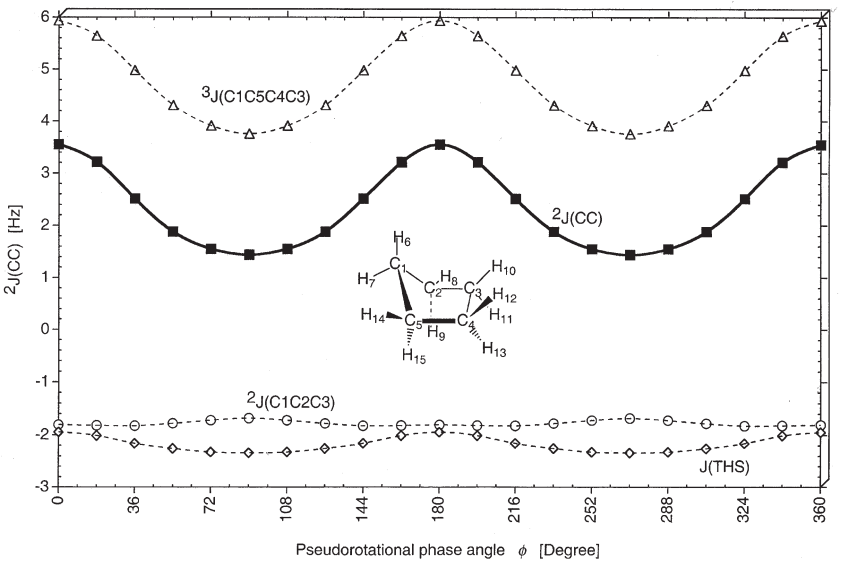

Fig. 4 Calculated geminal SSCCs $^2J(CC) = {}^2J(C1C3)$ of cyclopentane as a function of the pseudorotational phase angle ϕ. The two THB path contributions $^2J(C1C2C3)$, $^3J(C1C5C4C3)$ and the THS contribution $J(THS)$ are also shown. All calculations at MBPT2/cc-pVTZ geometries.

symmetry of the planar cyclopentane (D_{5h}) and planar THF (C_{2v}), which means that puckered cyclopentane forms with $\phi = 0 \pm \Delta\psi$ and $\phi = 90 \pm \Delta\psi$ are identical for unsubstituted cyclopentane and puckered THF forms with $\phi = 0 \pm \Delta\psi$ and $\phi = 180 \pm \Delta\psi$ identical for unsubstituted THF (see Fig. 3). For the calculation of the SSCCs there are just three unique E ($\phi = 0,36,72°$), three unique T forms ($\phi = 18,54,90°$), and the planar form ($q = 0$, ϕ not specified), which have to be considered. Of course, this minimum set of conformations can be augmented, if necessary, by setting the phase angle to other values than those of the T and E forms.

Cyclopentane and THF (see Scheme 1) possess pseudo rotational barriers equal or close to zero and therefore all measured SSCCs are averages over the pseudorotational mode.[35,36,45] The calculated average value of $\langle {}^2J(C2C5)\rangle$ is 2.33 Hz for cyclopentane, which agrees well with $\langle {}^2J(C,C)\rangle = 2.8$ Hz measured for methylcyclopentane.[35,40] The corresponding values for methylcyclobutane (−8.1 Hz) and methylcyclohexane (−1.6 Hz) are both negative[40] suggesting that geminal coupling in the five-membered ring must follow a different coupling mechanism. For the purpose of unraveling this mechanism, the geminal SSCC ^2J(C2C5) was calculated for a number of conformations along the pseudorotation path (for details of these calculations, see ref. 35) and plotted as a function of the pseudorotational angle ϕ (see Fig. 4 and Table 2).

Table 2 Different path contributions to the geminal NMR spin–spin coupling constants ^2J(CC) of cyclopentane[a]

ϕ	Through-space path	Two-bond path	Three-bond path	$\sum$	PI	Total
0	−1.95	−1.81	5.94	2.18	1.37	3.55
18	−2.01	−1.82	5.64	1.81	1.40	3.21
36	−2.16	−1.83	4.98	1.00	1.41	2.51
54	−2.26	−1.78	4.31	0.27	1.61	1.88
72	−2.33	−1.72	3.91	−0.14	1.69	1.55
90	−2.34	−1.68	3.76	−0.27	1.71	1.44

[a] The pseudorotational path angle ϕ gives the type of ring puckering. Compare with Fig. 3. Due to the D_{5h}-symmetry of planar cyclopentane, only $0 \le \phi \le 90°$ has to be considered. The through-space and the through-bond paths are shown in Fig. 1. $\sum$ stands for the sum of THS and THB contributions. PI gives the contribution resulting from the interactions between different paths. All SSCCs in Hz.

All geminal SSCCs ^2J(C2C5) are positive varying between 1.4 and 3.5 Hz. Each ^2J(C2C5) value was decomposed into THS, two-bond path, three-bond path, and PI contribution (Table 2, Fig. 4). The THS and the two-bond path contribution are both negative (as they should be, see discussion above) and are fairly constant during pseudorotation varying only by 0.4 and 0.15 Hz, respectively as is shown in Fig. 4. The PI contribution is 1.45 Hz ± 0.2 Hz for all conformations considered, which means that sign and magnitude of ^2J(C2C5) are determined by the positive three-bond path contribution, which varies between 3.9 and 5.9 Hz. Hence, the geminal CCC coupling in cyclopentane contains actually more vicinal CCCC coupling, which depends on the associated dihedral angle τ(C2C3C4C5). The latter adopts a zero value for $\phi = 0$, 180° and accordingly leads to a relatively large *cis* SSCC of 5.9 Hz while for $\phi = 90°$, τ becomes large (*ca.* 42°) and the three-bond path contribution is reduced to 3.8 Hz.

In cyclohexane and cyclobutane, both the three-bond path contribution does not exist. For cyclobutane, the two equivalent two-bond path contributions lead to a strong negative value of the geminal SSCC $^2|J|$(CC)(−8.1 Hz[40]) whereas for cyclohexane a small four-bond path contribution is dominated by the negative two-bond path contribution thus leading to a negative geminal CC SSCC (−1.6 Hz[40]).

In THF, the calculated geminal SSCCs $\langle {}^2J(C2C5)\rangle$ and $\langle {}^2J(C2C4)\rangle$ are 0.93 and 0.29 Hz.[36] Calculation of the actual values along the pseudorotation path reveals (see Fig. 5a) that ^2J(C2C4) contrary to the corresponding SSCC of cyclopentane can be both negative and positive. This is surprising because one would expect that ^2J(C2C4) (apart from the inductive effect of the O atom) resembles the corresponding cyclopentane SSCC most closely. Analysis of the path contributions (Fig. 5a and Table 3) reveals that this cannot be the case.

Again the THS, two-bond path, and the PI contribution are fairly constant although the effect of the O atom is reflected by the magnitude of these contributions. It is the three-bond path contribution (Fig. 5a, Table 3) that is responsible for the positive and negative values of ^2J(C2C4) and its small average value. The three-bond path contribution is dominated by a steric exchange contribution between the C2O1 and the C5C4 bond, which changes with the dihedral angle τ(C2O1C5C4) between them (small τ(C2O1C5C4) values imply a large ^3J(C2O1C5C4) value and *vice versa*, Fig. 5c).

For ^2J(C2C5) the THS and the two-bond path contributions become more negative, which is due to a negative lone pair

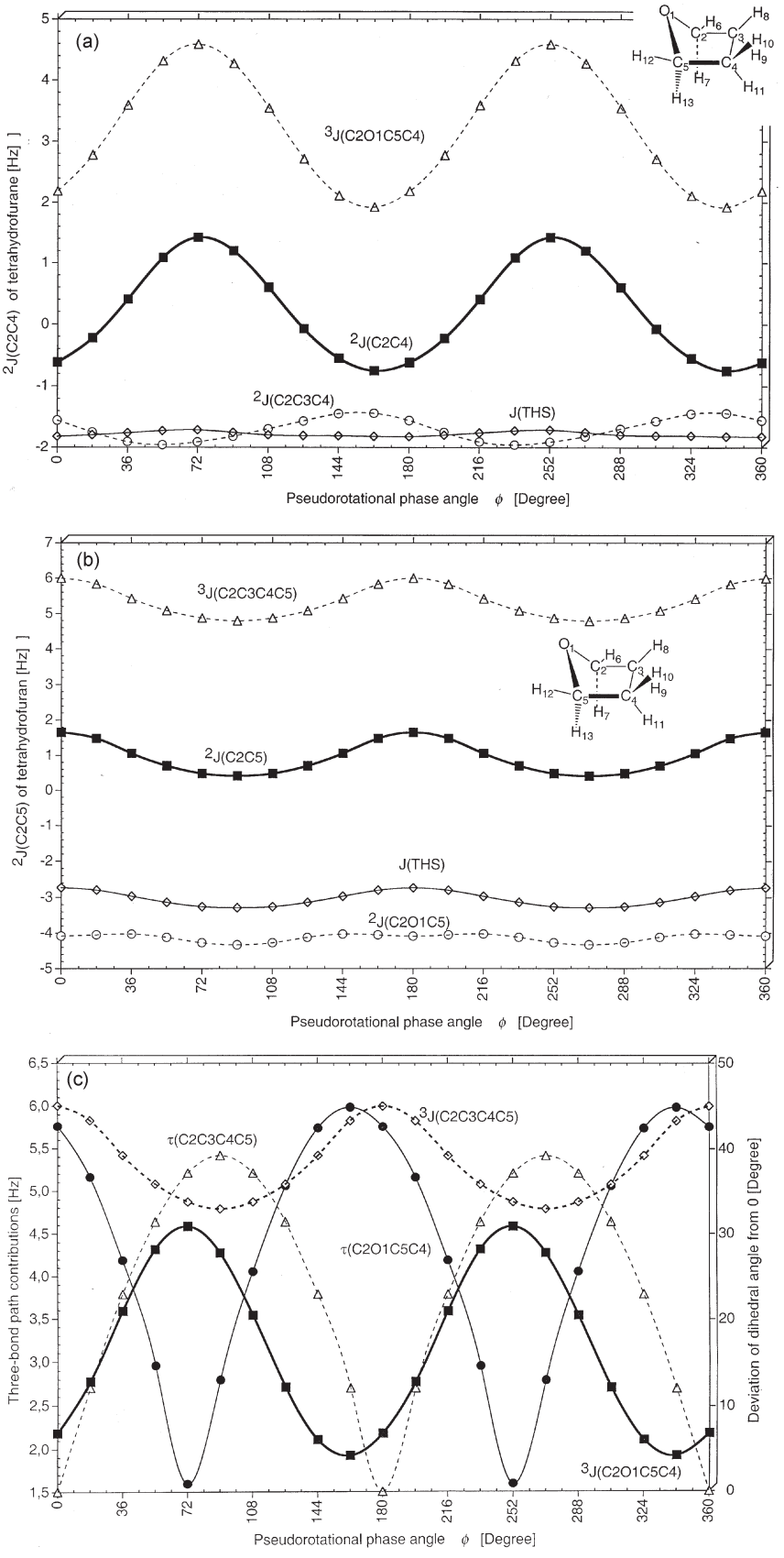

Fig. 5 (a) Calculated geminal SSCCs ^2J(C2C4) of tetrahydrofuran as a function of the pseudorotational phase angle ϕ. The two THB path contributions ^2J(C2C3C4), ^3J(C2O1C5C4) and the THS contribution J(THS) are also shown. (b) Calculated geminal SSCCs ^2J(C2C5) of tetrahydrofuran as a function of the pseudorotational phase angle ϕ. The two THB path contributions ^2J(C2O1C5), ^3J(C2C3C4C5) and the THS contribution J(THS) are also shown. (c) Three-bond contributions to the geminal SSCCs of tetrahydrofuran, ^2J(C2C5) and ^2J(C2C4) as a function of the pseudorotational phase angle ϕ. Also shown are the dihedral angles τ(C2C3C4C5) and τ(C2O1C5C4) as functions of ϕ.

Table 3 Different path contributions to the geminal NMR spin–spin coupling constants ^2J(CC) of tetrahydrofuran[a]

ϕ	Through-space path	Two-bond path	Three-bond path	$\sum$	PI	Total
^2J(C2C4)						
0	−1.82	−1.55	2.19	−1.19	0.57	−0.62
18	−1.79	−1.75	2.78	−0.77	0.55	−0.22
36	−1.76	−1.91	3.59	−0.07	0.49	0.41
54	−1.72	−1.96	4.32	0.64	0.45	1.09
72	−1.71	−1.91	4.59	0.97	0.45	1.42
90	−1.75	−1.82	4.28	0.71	0.49	1.20
108	−1.79	−1.69	3.55	0.06	0.54	0.60
126	−1.80	−1.56	2.71	−0.65	0.58	−0.07
144	−1.81	−1.44	2.11	−1.14	0.59	−0.55
162	−1.82	−1.44	1.93	−1.33	0.48	−0.75
180	−1.82	−1.55	2.19	−1.19	0.57	−0.62
^2J(C2C5)						
0	−2.73	−4.08	6.00	−0.81	2.46	1.65
18	−2.80	−4.05	5.83	−1.01	2.49	1.48
36	−2.97	−4.02	5.42	−1.57	2.63	1.06
54	−3.14	−4.11	5.08	−2.17	2.87	0.70
72	−3.26	−4.27	4.87	−2.65	3.13	0.48
90	−3.29	−4.33	4.79	−2.82	3.23	0.41

[a] The pseudorotational path angle ϕ gives the type of ring puckering. Compare with Fig. 3. Due to the C_{2v}-symmetry of planar THF, only $0 \leq \phi \leq 180°$ has to be considered. As for the numbering of atoms compare with Scheme 1. $\sum$ stands for the sum of THS and THB contributions. PI gives the contribution resulting from the interactions between different paths. All SSCCs in Hz.

contribution according to the *J*-**OC**-PSP analysis. As in cyclopentane, they are always negative with small but non-negligible variation in dependence of ϕ (see Fig. 5b). The difference between two-bond components, ^2J(C2C3C4) and ^2J(C2O1C5) (2.0–2.9 Hz, Table 3) is comparable to the difference of 1.6 Hz found for ^2J(CC) of propane (−0.68 Hz) and ^2J(CC) for ether (−2.35 Hz).[40] The PI varies between 2.5 and 3.2 Hz and is more than 2 Hz larger than in the case of the SSCC ^2J(C2C4), which again reflects the strong influence of the electron lone pair at O on the ^3J(C2C3C4C5) SSCC by steric exchange repulsion with bonds C3H and C4H.

In the same manner as for ^2J(C2C4), the variations of ^2J(C2C5) are dominated by the three-bond contributions (see Fig. 5b), which correlate with the dihedral angle, τ(CXCC) of the corresponding fragments (Fig. 5c). The more the dihedral angle deviates from 0°, the smaller are the three-bond contributions. Therefore, J(C2C5) adopts large values for $\phi = 0$, 180°, while J(C2C4) adopts large values for $\phi = 72$, 252° (Fig. 5).

V. Conclusions

The analysis of measured multipath SSCCs requires the application of theoretical methods such as the one used in this work. The *J*-**OC**-PSP analysis of calculated multipath SSCCs reveals that the coupling mechanism includes through-space and two or more through-bond contributions. Additivity of suitable increments will only be given if the path interaction terms are small. Path interactions increase in magnitude when there are strong steric exchange interactions between the various paths. The sign of the THS contributions can be predicted with the help of the Fermi contact spin density distribution calculated from the localized molecular orbitals involved in the coupling mechanism. In this way, the unusual SSCC J(C4C5) = −26.1 Hz of bicyclo[1.1.1]pentane is explained as a result of a through-space interaction (−2.6 Hz) between the two bridgehead atoms, which itself is the sum of two opposing through-space contributions (THS paths 1 and 2 in Fig. 1e), three equivalent two-bond interactions (−4.4 Hz, Fig. 1d), and a large path interaction term of −10.2 Hz resulting from steric exchange repulsion between three bridging CH_2 groups.

For cyclopropane, the one-bond contribution ^1J(CC) is 54.4 Hz as it should be for a CC bond with substantial π character. Through-space (−27.1 Hz) and two-bond contribution (10.1 Hz) lead in sum to a typical geminal SSCC of a strongly strained carbon ring (−17.1 Hz). The path interaction term is −24.5 Hz reflecting the strong interaction between the CC bond orbitals in the three-membered ring. The total SSCC is reduced by the two-bond and the PI contribution to 12.9 Hz, which is in good agreement with the experimental value of 12.4 Hz.[40]

Measured and calculated ^2J(CC) coupling constants of cyclopentane and tetrahydrofuran are shown to be averages over the pseudorotational motion of these ring molecules where each individual SSCC of a conformation passed in the pseudorotation is the sum of a THS, a two-bond path, a three-bond path, and a PI contribution. THS, two-bond path and PI contribution vary only slightly during pseudorotation. The Karplus relationship for ^2J(CC) = f(ϕ) of cyclopentane and THF discussed in the literature[35,36] is a result of the dependence of the three-bond contribution on the associated dihedral angle τ(CCCC), which in turn depends on the pseudorotational phase angle ϕ. The clarification of these relationships helps the conformational analysis of pseudorotating ring molecules along the lines of the recently developed DORCOR (determination of ring conformations) method.[45]

Acknowledgements

This work was supported at Gothenburg by the Swedish Natural Science Research Council (NFR). Calculations were done on the supercomputers of the Nationellt Superdatorcentrum (NSC), Linköping, Sweden. DC thanks the NSC for a generous allotment of computer time.

References

1 See, *e.g.*, *Encyclopedia of Nuclear Magnetic Resonance*, ed. D. M. Grant and R. K. Harris, Wiley, Chichester, UK, 1996, vol. 1–8.
2 (*a*) J. Kowalewski, *Prog. NMR Spectrosc.*, 1977, **11**, 1–78; (*b*) J. Kowalewski, *Annu. Rep. NMR Spectrosc.*, 1982, **12**, 81–176.
3 R. H. Contreras and J. E. Peralta, *Prog. NMR Spectrosc.*, 2000, **37**, 321.
4 L. B. Krivdin and E. W. Della, *Prog. NMR Spectrosc.*, 1990, **23**, 301.
5 R. H. Contreras and J. C. Facelli, *Annu. Rep. NMR Spectrosc.*, 1993, **27**, 255.
6 J. L. Marshall, S. R. Walter, M. Barfield, A. P. Marchand, N. W. Marchand and A. L. Segre, *Tetrahedron*, 1976, **32**, 537.
7 J. L. Marshall, L. G. Faehl and R. Kattner, *Org. Magn. Reson.*, 1979, **12**, 163.
8 M. Klessinger and M. Stöcker, *Org. Magn. Reson.*, 1981, **17**, 97.
9 M. Klessinger and J. H. Cho, *Angew. Chem.*, 1982, **94**, 782.
10 M. Klessinger, H. van Megen and K. Wilhelm, *Chem. Ber.*, 1982, **115**, 50.
11 M. Klessinger and J. H. Cho, *Org. Magn. Reson.*, 1983, **21**, 465.
12 J. H. Cho, M. Klessinger, U. Tecklenborg and K. Wilhelm, *Magn. Reson. Chem.*, 1985, **23**, 95.
13 G. E. Scuseria, J. C. Facelli, R. H. Contreras and A. R. Engelmann, *Chem. Phys. Lett.*, 1983, **96**, 560.
14 R. H. Contreras and G. E. Scuseria, *Org. Magn. Reson.*, 1984, **22**, 411.
15 G. A. Aucar, V. Zunino, M. B. Ferraro, C. G. Giribet, M. C. Ruiz de Azua and R. H. Contreras, *J. Mol. Struct. (THEOCHEM)*, 1990, **205**, 63.

16 G. A. Aucar, M. C. Ruiz de Azua, C. G. Giribet and R. H. Contreras, *J. Mol. Struct. (THEOCHEM)*, 1990, **205**, 79.
17 M. Stöcker, *Org. Magn. Reson.*, 1982, **20**, 175.
18 A. R. Engelmann and R. H. Contreras, *Int. J. Quantum Chem.*, 1983, **23**, 1033.
19 (*a*) H. Fukui, K. Miura, H. Matsuda and T. Baba, *J. Chem. Phys.*, 1992, **97**, 2299; (*b*) T. Helgaker, M. Jaszunski and K. Ruud, *Chem. Rev.*, 1998, **99**, 293; (*c*) H. Fukui, *Prog. NMR Spectrosc.*, 1999, **35**, 267.
20 (*a*) A. Laaksonen, J. Kowalewski and V. R. Saunders, *Chem. Phys.*, 1983, **80**, 221; (*b*) O. Vahtras, H. Ågren, P. Jørgensen, J. J. Aa. Jensen, T. Helgaker and J. Olsen, *J. Chem. Phys.*, 1992, **96**, 2118; 1992, 97, 9178.
21 (*a*) J. Gauss and J. F. Stanton, *Chem. Phys. Letters*, 1997, **276**, 70; (*b*) A. A. Auer and J. Gauss, *J. Chem. Phys.*, 2001, **115**, 1619.
22 V. Sychrovský, J. Gräfenstein and D. Cremer, *J. Chem. Phys.*, 2000, **113**, 3530.
23 N. F. Ramsey, *Phys. Rev.*, 1953, **91**, 303.
24 (*a*) A. D. Becke, *J. Chem. Phys.*, 1993, **98**, 5648; (*b*) A. D. Becke, *Phys. Rev. A*, 1988, **38**, 3098; (*c*) C. Lee, W. Yang and R. P. Parr, *Phys. Rev. B*, 1988, **37**, 785.
25 (*a*) V. Polo, E. Kraka and D. Cremer, *Mol. Phys.*, 2002, **100**, 1771; (*b*) V. Polo, E. Kraka and D. Cremer, *Theor. Chem. Acc.*, 2002, **107**, 291; (*c*) V. Polo, J. Gräfenstein, E. Kraka and D. Cremer, *Chem. Phys. Lett.*, 2002, **352**, 469; (*d*) V. Polo, J. Gräfenstein, E. Kraka and D. Cremer, *Theor. Chem. Acc.*, 2003, **109**, 22.
26 A. Wu and D. Cremer, *J. Phys. Chem.*, in press.
27 A. Wu and D. Cremer, *J. Am. Chem. Soc.*, submitted.
28 (*a*) W. Kohn and L. Sham, *Phys. Rev. A*, 1965, **140**, 1133; For reviews on DFT, see for example(*b*) R. G. Parr and W. Yang, *International Series of Monographs on Chemistry 16: Density-Functional Theory of Atoms and Molecules*, Oxford University Press, New York, 1989; (*c*) *Density Functional Methods in Chemistry*, eds. J. K. Labanowski and J. W. Andzelm, Springer, Heidelberg, 1990; (*d*) *Theoretical and Computational Chemistry, Vol. 2, Modern Density Functional Theory - A Tool for Chemistry*, eds. J. M. Seminario and P. Politzer, Elsevier, Amsterdam, 1995; (*e*) *Chemical Applications of Density Functional Theory*, ACS Symposium Series 629, eds. B. B. Laird, R. B. Ross and T. Ziegler, American Chemical Society, Washington, DC, 1996; (*f*) *Recent Advances in Computational Chemistry Vol. 1, Recent Advances in Density Functional Methods Part II*, ed. D. P. Chong, World Scientific, Singapore, 1997.
29 (*a*) P. C. Hariharan and J. A. Pople, *Theor. Chim. Acta.*, 1973, **28**, 213.
30 For a recent review see, D. Cremer, in *Encyclopedia of Computational Chemistry*, ed. P. v. R. Schleyer, N. L. Alinger, T. Clark, J. Gasteiger, P. A. Kollman, H. F. Schaefer and P. R. Schreiner, Wiley, Chichester, UK, vol. 3, p. 1706.
31 T. H. Dunning, Jr., *J. Chem. Phys.*, 1989, **99**, 107.
32 D. Cremer andPople, *J. Am. Chem. Soc.*, 1975, **97**, 1354.
33 D. Cremer and K. J. Szabo, *Methods in Stereochemical Analysis, Conformational Behavior of Six-Membered Rings, Analysis, Dynamics, and Stereoelectronic Effects*, ed. E. Juaristi, VCH Publishers, 1995, 59.
34 D. Cremer, *J. Phys. Chem.*, 1990, **94**, 5502.
35 A. A. Wu, D. Cremer, A. A. Auer and J. Gauss, *J. Phys. Chem. A*, 2002, **106**, 657.
36 A. Wu and D. Cremer, *Int. J. Mol. Sci.*, 2003, **4**, 158.
37 W. Kutzelnigg, U. Fleischer and M. Schindler, in *NMR—Basic Principles and Progress*, Springer, Heidelberg, 1990, 23, 165.
38 E. Kraka, J. Gräfenstein, M. Filatov, Y. He, J. Gauss, A. Wu, V. Polo, L. Olsson, Z. Konkoli, Z. He and D. Cremer, *COLOGNE 2003*, Gothenburg University, Sweden, 2003.
39 M. J. Frisch, G. W. Trucks, H. B. Schlegel, G. E. Scuseria, M. A. Robb, J. R. Cheeseman, V. G. Zakrzewski, J. A. Montgomery, Jr., R. E. Stratmann, J. C. Burant, S. Dapprich, J. M. Millam, A. D. Daniels, K. N. Kudin, M. C. Strain, O. Farkas, J. Tomasi, V. Barone, M. Cossi, R. Cammi, B. Mennucci, C. Pomelli, C. Adamo, S. Clifford, J. Ochterski, G. A. Petersson, P. Y. Ayala, Q. Cui, K. Morokuma, D. K. Malick, A. D. Rabuck, K. Raghavachari, J. B. Foresman, J. Cioslowski, J. V. Ortiz, B. B. Stefanov, G. Liu, A. Liashenko, P. Piskorz, I. Komaromi, R. Gomperts, R. L. Martin, D. J. Fox, T. Keith, M. A. Al-Laham, C. Y. Peng, A. Nanayakkara, C. Gonzalez, M. Challacombe, P. M. W. Gill, B. Johnson, W. Chen, M. W. Wong, J. L. Andres, C. Gonzalez, M. Head-Gordon, E. S. Replogle and J. A. Pople, *Gaussian 98, Revision A.5*, Gaussian, Inc., Pittsburgh PA, 1998.
40 H. O. Kalinowski, S. Berger and S. Braun, *^{13}C-NMR-Spektroskopie*, Georg Thieme Verlag, Stuttgart, 1984, and references cited therein.
41 M. Barfield, S. E. Brown, E. D. Canada, Jr., N. D. Ledford, J. L. Marshall, S. R. Walter and E. Yakali, *J. Am. Chem. Soc.*, 1980, **102**, 3355.
42 J. L. Marshall, *Carbon-carbon and carbon-proton NMR couplings: Applications to Organic Stereochemistry and Conformational Analysis*, VCH, Deerfield Beach, FL, 1983.
43 A. P. Marchand, *Stereochemical Application of NMR studies in Rigid Bicyclic Systems*, VCH, Deerfield Beach, FL, 1982.
44 D. Cremer, E. Kraka and K. J. Szabo, in *The Chemistry of Functional Groups, The Chemistry of the Cyclopropyl Group*, ed. Z. Rappoport, Wiley, New York, 1995, vol. 2, p. 43–137.
45 A. Wu and D. Cremer, *J. Phys. Chem. A*, 2003, **107**, 1797.